The Interfacial Region of Dipalmitoylphosphatidylcholine Bilayers Is Perturbed by Fusogenic Amphipaths

Barry R. Lentz, Jogin R. Wu, LianXing Zheng, and Jan Převrátil
Department of Biochemistry and Biophysics, University of North Carolina at Chapel Hill, Chapel Hill, North Carolina 27599-7260 USA

ABSTRACT Several structural methods were used to probe the influence of three fusogenic and four nonfusogenic amphipaths on large, unilamellar dipalmitoylphosphatidylcholine (DPPC) vesicles. For four of these structural measurements there was a correlation observed between the ability of an amphipath to favor poly(ethylene glycol) (PEG)-induced fusion and the structural perturbation reported by each method. First, the fluorescence anisotropy of 1-[4-(trimethylamino)phenyl]-6-phenyhexa-1,3,5-triene (TMA-DPH), which probes the upper region of the bilayer, decreased in the range of PEG concentrations previously found to cause fusion of membranes containing fusogenic amphipaths. For nonfusogenic amphipaths, the anisotropy increased monotonically with PEG concentration. The properties of similar probes that locate in the hydrophobic core of the bilayer showed no correlation with fusogenicity, nor did the properties of probes purported to sense the aqueous surface of the membrane. Second, the frequency of the C=O stretch increased and then decreased dramatically as fusogenic but not nonfusogenic membranes were heated through their phase transition. Third, there was a dramatic increase in the frequency of the C-O-C ester stretch at the membrane order/disorder phase transition for membranes containing fusogenic amphipaths, twice the increase observed for nonfusogenic amphipaths. The spectral characteristics of phosphate, choline, and acyl chain motions showed no such correlation with fusogenicity. Finally, calorimetric measurements showed that low levels of fusogenic amphipaths eliminated the "pretransition" ($L_\beta \rightarrow P_{\beta'}$) in DPPC membranes, whereas other amphipaths shifted but did not eliminate this transition. Taken together, these results indicate that fusogenic amphipaths perturb the interface or "backbone" region of the bilayer rather than the hydrophobic core, the headgroup, or the water interface regions of DPPC bilayers.

INTRODUCTION

Fusion of vesicular membrane mimetopes by poly(ethylene glycol) (PEG) has for some time been a popular model system for examining the phenomenon of membrane fusion (Lentz, 1994). This model system has the advantage that the aggregation and fusion processes can be separated; indeed, PEG can force phosphatidylcholine bilayers to a point of molecular contact between bilayers without forcing fusion (Burgess et al., 1991, 1992). Fusion occurs only when vesicle bilayer membranes are perturbed in some way: through the inclusion of certain amphipathic molecules, through the induction of high bilayer curvature, or by including in the vesicle membrane a mixture of lipids with different molecular shapes (Lentz et al., 1992; Burgess et al., 1992; Wu et al., 1996). Although it is not known what all of these perturbing effects have in common, it seems likely that all disrupt in some way the structure of the lipid bilayer. The exact nature of this fusion-generating disruption is unknown. It is likely that any amphipathic molecule added to a regularly packed dipalmitoylphosphatidylcholine (DPPC) bilayer will alter bilayer structure in some way, but not all amphipaths examined have the effect of inducing fusion (Lentz et al., 1992). Indeed, lysophosphatidylcholine has been shown to induce PEG-mediated fusion of DPPC large, unilamellar vesicles (LUVETs) (Lentz et al., 1992) but has been reported to inhibit the fusion of biological membranes when added from the extracytoplasmic face (Chernomordik et al., 1993). Indeed, in black lipid membranes and in LUVETS, lysophophatidylcholine has been shown to have different effects, depending onto which bilayer leaflet it has been added (Chernomordik et al., 1995; Wu et al., 1996).

In this report we concentrate our efforts on locating the perturbing influence of fusion-inducing amphipaths in one or more regions of the membrane bilayer and defining the nature of this perturbation. We have done this by probing and contrasting the influence of fusogenic and nonfusogenic amphipaths on the four principal bilayer regions (the water layer next to the polar region, the polar head region, the interface region containing the esterified glycerol backbone, and the hydophobic region containing the fatty acid acyl chains). To this end, we have employed several different fluorescent probes, Fourier transform infrared (FTIR) spectroscopy, and differential scanning calorimetry (DSC). The results show that fusogenic amphipaths were distinct from nonfusogenic ones in that all perturb the structure of the interface region of the bilayer. Fusogenic and nonfusogenic amphipaths were not distinguishable through their effects on other regions of the bilayer. Unfortunately, the nature of the fusion-competent structural change cannot be defined from our data.

Received for publication 8 July 1996 and in final form 10 September 1996.
Address reprint requests to Dr. Barry R. Lentz, Department of Biochemistry and Biophysics, University of North Carolina at Chapel Hill, Chapel Hill, NC 27599-7260. Tel.: 919-966-5384; Fax: 919-966-2852; E-mail: uncbrl@med.unc.edu.

0006-3495/96/12/3302/09 $2.00

MATERIALS AND METHODS

1,2-Dipalmitoyl-3-*sn*-phosphatidylcholine (DPPC) in a chloroform stock solution was purchased from Avanti Polar Lipids (Birmingham, AL). DPPC stocks were filtered over Norit A neutral activated charcoal to remove trace fluorescent contaminants. All lipids were found to be greater than 98% pure by thin-layer chromatography on Analtech (Newark, DL) GHL silica gel plates poured in the presence of 0.01 M dipotassium oxalate. Plates were developed in a 65:25:4 (v/v/v) $CHCl_3$:CH_3OH:H_2O mixture, and lipids were visualized with iodine vapor. 1-Monooleoyl-*rac*-glycerol (MOG), 1,2-dipalmitoylglycerol (DPG), 1,2-dioleoyl-*sn*-glycerol (DOG), 1-oleoyl-2-acetyl-*sn*-glycerol (OAG), L-α-lysopalmitoylphosphatidylcholine (LPC), and stearyl amine were purchased from Sigma Chemical Company (St. Louis, MO). Palmitic acid (PA) was purchased from Nu Chek Prep (Elysian, MN). Platelet activating factor (C_{16} species; PAF) was purchased from Boehringer Mannheim Biochemicals (Indianapolis, IN). *N*-[Tris(hydroxymethyl)methyl]-2-aminoethanesulfonic acid (TES) was purchased from Research Organics (Cleveland, OH), and 3-(*N*-morpholino)propanesulfonic acid (MOPS) was obtained from Sigma Chemical Company. 1,6-Diphenyl-1,3,5-hexatriene (DPH), 1-[4-(trimethylamino-)phenyl]-6-phenylhexa-1,3,5-triene (TMA-DPH), (2-carboxyethyl)-1,6-diphenyl-1,3,5-hexatriene (CE-DPH), 1–4-nitrobenzo-2-oxa-1,3-diazole-phosphatidylethanolamine (NBD-PE), and dansylphosphatidylethanolamine (DPE) were obtained from Molecular Probes (Junction City, OR). All other reagents were of the highest quality available.

Methods

Extruded vesicles were prepared by the procedure of Mayer et al. (1986) with some modifications. Lipid components (DPPC stock solution and appropriate amounts of amphipath stock solutions) were mixed in chloroform solution, and the solvent was removed under a stream of nitrogen or argon. The lipid residue was redissolved in cyclohexane and frozen in a dry ice/acetone bath, and the solvent was removed under high vacuum to yield a white powder. The dried lipid was hydrated in the appropriate prewarmed buffer at 45–48°C before extrusion. The buffer for fluorescence and FTIR studies contained 150 mM NaCl, 10 mM TES (pH 7.4), whereas that for DSC experiments contained 150 mM NaCl, 50 mM MOPS (pH 7.4). The resulting multilamellar vesicles were forced seven times through a 0.1-μm polycarbonate filter (Nucleopore, Cambridge, MA) by argon at a pressure of about 200 psi. The concentrations of all vesicle samples were determined by phosphate analysis, by the modified procedure of Chen et al. (1956).

Fluorescence measurements were made at 48°C using an SLM 48000 spectrofluorometer (SLM-Aminco, Rochester, NY) equipped with a Photon Technology International light source (model A1010; Princeton, NJ) with horizontally mounted 200-W Hg-xenon or 150-W xenon arc lamps. The fluorescence anisotropy of DPH and DPH-containing probes was measured with the T format with excitation set at 366 nm (slit = 4), and emission was measured using a 450-nm cutoff filter (Schot Optical Glass, Duryea, PA). The fluorescence anisotropy of NBD-PE was measured with excitation at 470 nm and emission at 530 nm (slits = 4). Estimates of membrane surface dielectric constant were made with DPE as described by Ohki and Arnold (1990). DPE was incorporated into vesicle membranes (phospholipid/DPE ~250) that were suspended in TES buffer at a concentration of 0.05 mM lipid for estimating the surface dielectric constant. The emission spectra of DPE were obtained in the range of 400–600 nm by exciting at 340 nm (xenon lamp), and the effective surface dielectric constant was estimated from the emission peak position by comparison to the peak position of this probe dissolved in a variety of organic solvents (15 μg/ml) with different bulk dielectric contstants (Ohki and Arnold, 1990).

Fluorescence lifetime and phase-resolved anisotropy measurements with TMA-DPH were made at 48°C using the SLM-48000 MHF spectrofluorometer with an excitation wavelength of 366 nm (UV light of a Innova 90–4 laser; Coherent, Palo Alto, CA) using a correlation frequency of 60 Hz and 300 data averaging. A base modulation frequency of 4 MHz was used with data collected at roughly 25 frequencies geometrically related to this base frequency (4–120 MHz for lifetimes; 4–100 MHz for anisotropy decay). The lipid:probe ratio and lipid concentration used were 250:1 and 0.2 mM, respectively. All lifetime measurements were obtained with glycogen as a reference. For lifetime measurements, exciting light was vertically polarized, and the polarizer in the emission channel was set at the magic angle (37.5°). Phase-resolved dynamic anisotropy measurements were performed using the T format. Data and error analyses were performed with the Globals Unlimited software package developed at the Laboratory for Fluorescence Dynamics, Department of Physics, University of Illinois (Urbana, IL).

FTIR spectra were measured on a Mattson Polaris FT-IR spectrometer equipped with a high-efficiency liquid nitrogen-cooled mercury-cadmium telluride detector. Samples made with H_2O buffer were delivered between CaF_2 windows separated by a 12-μm-thick spacer and located in a Harrick flow-through cell thermostated by a temperature-controlled Haake Water Bath (Haake Inc., Saddle Brook, NJ) that gives a temperature stability of better than 0.1°C. The temperature was monitored directly by a copper-constantan thermocouple located against the cell window. To obtain a spectrum at each temperature, 500 scans were co-added, at a spectral resolution of 4 cm^{-1}. All spectral analyses were performed using LabCalc software (Galactic Industries Corporation, Salem, NH).

Differential scanning calorimetry (DSC) was performed on a Microcal (Amherst, MA) MC-2 biological microcalorimeter equipped with a Keithly 150B amplifier. Samples (1.18 ml) were degassed under reduced pressure (~100 mm Hg) for 30 min before being loaded into the calorimeter cell with a Hamilton microliter/gastight syringe. Samples were suspended in MOPS buffer at a concentration of 3 mM. The scan rate for all experiments was 20°C/h. Data (voltage proportional to sample heat capacity) were recorded every 5 s directly to an interfaced personal computer using software supplied by Microcal. Calorimetric data were converted to heat capacity (kcal mol^{-1} $°C^{-1}$) versus temperature, also by Microcal software. Multiple peaks were resolved using a deconvolution algorithm supplied by Microcal that assumed independent, non-two-state transitions.

RESULTS AND DISCUSSION

Fluorescence probe measurements

As a first attempt at detecting distinctive structural perturbations induced by amphipaths, we compared the steady-state fluorescence anisotropy of four fluorescent probes, each of which senses molecular motion in a different region of the bilayer. In Fig. 1 we present the fluorescence anisotropy of these probes as a function of the concentration of PEG added to DPPC LUVET containing different amphipaths. Not surprisingly, the anisotropies of each probe increased with PEG concentration, presumably because of the increased viscosity of PEG solutions. In membranes containing LPC (*open squares*) and PA (*open inverted triangles*), however, TMA-DPH displayed a sudden and measurable decrease in fluorescence anisotropy at and above 30 wt% PEG, the concentration at which fusion was first observed in the presence of these amphipaths (Lentz et al., 1992). Neither pure DPPC LUVETs (*open circles*) nor LUVETs containing nonfusogenic amphipaths (DOG, *open triangles*; OAG, *open diamonds*) showed this behavior. TMA-DPH probes the uppermost hydrophobic region of the bilayer, just below the interface or glycerol backbone region (Ho et al., 1995). Probes that sensed the structure of bilayer regions other than the interface region (DPH, the hydrophobic core; CE-DPH, the mid-hydrophobic region; NBD-PE, the headgroup region) reported no difference between the

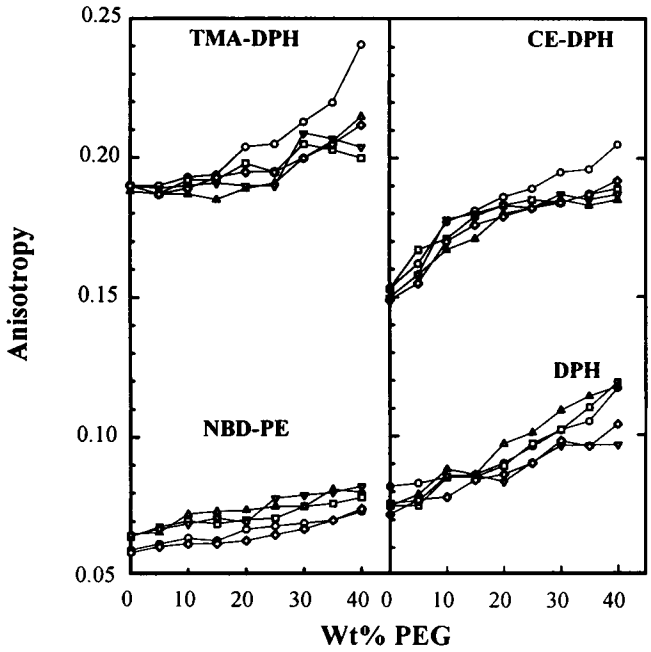

FIGURE 1 Steady-state fluorescence anisotropy of TMA-DPH, NBD-PE, CE-DPH, and DPH associated with DPPC LUVET as a function of the concentration of PEG added to LUVET suspensions. Measurements are presented for DPPC membranes alone (○) and membranes containing 0.5 mol% fusogenic (LPC, □; PA, ▽) and nonfusogenic (DOG, △; OAG, ◇) amphipaths (lipid/probe ~250, 0.2 mM lipid).

effects of fusogenic and nonfusogenic amphipaths. These results suggest that there is some difference in the interface region structure in membranes containing fusogenic versus nonfusogenic amphipaths. The detailed nature of this difference is not clear from these steady-state anisotropy data.

To better define the structural distinction between membranes containing fusogenic versus nonfusogenic amphipaths, we attempted to measure the dynamics of TMA-DPH fluorescence. It was found that phase shift and modulation ratio data for TMA-DPH in DPPC vesicles in the absence of PEG could not be described in terms of a single lifetime component (reduced χ^2 = 175), but could be described adequately by assuming two lifetime components (reduced χ^2 = 1.5). These two-lifetime descriptions are summarized in Table 1. As can be seen from the table, the presence of fusogenic (LPC) or nonfusogenic (DOG) amphipaths had no discernible effect on the fluorescence lifetime of TMA-DPH, at least in the absence of PEG. In the presence of PEG, the description of TMA-DPH fluorescence decay in terms of two lifetime components was more tenuous but still served as a first approximation. The contribution of the short lifetime component increased as the PEG concentration increased for all three vesicle systems. The lifetime associated with this component also decreased, so the average liftime decreased. However, as was the case in the absence of PEG, there was no discernible influence of amphipaths on the TMA-DPH lifetime description in the presence of PEG.

To determine whether motional properties of TMA-DPH were able to distinguish between vesicles prepared in the presence of fusogenic versus nonfusogenic amphipaths, differential polarized phase shifts and modulation ratios collected using the SLM-Aminco 48000 MHF spectrofluorometer were analyzed according to two different models of probe motion; the results are summarized in Tables 2 and 3. The first model was the "wobble in a cone" model, most often applied to this type of membrane probe (Kinosita et al., 1977). The second model used was the "bimodal orien

TABLE 1 TMA-DPH fluorescence lifetime analysis

Vesicles	[PEG] %w/w	f_1	τ_1	f_2	τ_2	$\Sigma f_i\tau_i$	χ^2
DPPC	0	0.848	3.532	0.152	0.844	3.123	1.517
		(0.870–0.825)	(3.456–3.621)	(0.175–0.131)	(0.968–0.694)		
	30	0.584	3.621	0.416	0.236	2.213	2.345
		(0.594–0.574)	(3.708–3.526)	(0.426–0.406)	(0.263–0.206)		
	40	0.364	4.158	0.636	0.148	1.608	5.822
		(0.375–0.352)	(4.390–3.891)	(0.647–0.624)	(0.171–0.121)		
DPPC + 0.5% DOG	0	0.874	3.429	0.126	0.726	3.088	0.380
		(0.883–0.864)	(3.463–3.398)	(0.135–0.117)	(0.789–0.658)		
	30	0.560	3.606	0.440	0.238	2.124	4.368
		(0.574–0.547)	(3.733–3.469)	(0.453–0.426)	(0.274–0.199)		
	40	0.370	3.759	0.630	0.177	1.502	3.348
		(0.380–0.360)	(3.921–3.579)	(0.640–0.620)	(0.197–0.156)		
DPPC + 0.5% LPC	0	0.857	3.471	0.143	0.823	3.092	0.612
		(0.870–0.843)	(3.518–3.426)	(0.157–0.131)	(0.901–0.735)		
	30	0.591	3.487	0.409	0.231	2.150	1.938
		(0.600–0.582)	(3.564–3.406)	(0.419–0.400)	(0.257–0.203)		
	40	0.359	3.762	0.641	0.168	1.458	2.609
		(0.368–0.350)	(3.910–3.600)	(0.649–0.632)	(0.185–0.150)		

The lifetime of TMA-DPH in DPPC vesicles at different concentration of PEG was obtained by fitting two linked phase shift and modulation ratio data sets with the Global Unlimited software. Fitting parameters are the two lifetimes (τ_1 and τ_2) and the intensity fraction of one of these two components (f_1, with $f_1 + f_2 = 1$).

TABLE 2 Analysis of frequency-resolved anisotropy data for TMA-DPH incorporated into DPPC LUVET assuming a single average probe lifetime

Model	[PEG] (%w/w)	θ (ns)	r_∞	*P2* weight	*P4* weight	D_{rot} (ns^{-1})	χ^2
Hindered cone	0	1.177	0.099				1.157
	30	2.723	0.043				8.218
	40	4.234	−0.004				22.343
P2-P4	0			0.488	0.356	0.114	0.767
	30			0.000	0.369	0.083	19.159
	40			0.000	0.546	0.141	38.571

TMA-DPH phase-resolved dynamic anisotropy data were fit using different models for probe motion, but always assuming one average probe fluorescence lifetime. r_0 was fixed at 0.34. Fitting parameters were the rotational correlation time for free rotation in a cone (θ), the long-time anisotropy (r_∞) related to the cone angle; the weighting factors for the two components (*P2*, *P4*) of the bimodal orientational distribution; and the rotational diffusion coefficient for rotation in this potential (D_{rot}).

tational potential" model (the "P2/P4" model; Zannoni et al., 1983; van der Meer et al., 1984), applied to DPH probes by Straume and Litman (1987). Both models assume a cylindrically symmetrical probe with excitation and emission dipoles parallel to the long axis and a single fluorescence decay time (Zannoni et al., 1983). Whereas the first two assumptions are troublesome for TMA-DPH (Lentz, 1993), the third assumption is clearly not valid (Table 1). The common approach to this complication in treating the decay of fluorescence anisotropy is to assume a single average lifetime (intensity weighted average, as described by Muller et al., 1994). We initially took this approach in fitting our differential polarized phase shift/modulation ratio data. We then used the ability of the Globals software package to account for multiple lifetime components to examine the importance of the average lifetime assumption.

The residuals resulting from fitting these two models to our data, with the assumption of assigning a single average decay time to TMA-DPH fluorescence, are summarized in Fig. 2, *A* and *B*, with parameters for these fits summarized in Table 2. Not surprisingly, the three-parameter "P2/P4" model provided a somewhat better fit than the two-parameter "cone" model, with the inadequacy of the cone model being most evident at low modulation frequencies. Others have shown that a single-lifetime, P2/P4 model will describe the differential phase and modulation data for TMA-DPH better than a cone model (Straum and Litman, 1987; van Langen, 1989). We pointed out (Lentz, 1993) that the distribution obtained from unconstrained P2/P4 fits of such data (see, e.g., Table 2) were unreasonable in predicting a significant probability of locating a TMA-DPH molecule lying in the plane of the membrane.

When the assumption of a single, average lifetime was relaxed to allow for the two measured lifetimes (Table 1), the simple "wobble in a cone" was clearly the preferred model, as it adequately described the data (Table 3 and Fig. 2, *C* and *D*) with one less parameter than the P2/P4 model, and without the unreasonable prediction of a probe population parallel to the membrane surface (as required by the P2/P4 model). Thus the nonexponential behavior of TMA-DPH fluorescence anisotropy decay can be attributed to the nonexponential decay of total TMA-DPH fluorescence combined with the simplest model for hindered probe rotation. Wang et al. (1991) have already pointed this out with respect to the interpretation of differential polarized phase and modulation data from DPH, although Chen et al. (1977) reported that time-resolved anisotropy data from DPH in membranes could not be fit with a single exponential, even when account was taken of the complication of two lifetime components. In this regard, we note that the model of the simple cone plus two lifetime components does not provide a perfect description of our phase and modulation data (note that the residuals in Fig. 2 *C*, although close to zero, are not completely randomly distributed). Breakdown of the other

TABLE 3 Analysis of frequency-resolved anisotropy data for TMA-DPH incorporated into DPPC LUVET assuming two probe lifetimes

Model	[PEG] (%w/w)	θ (ns)	r_∞	*P2*	*P4*	D_{rot}	χ^2
Hindered cone	0	0.993	0.097				0.769
	30	0.734	0.099				11.637
	40	0.513	0.102				18.643
P2-P4	0			0.533	0.193	0.121	0.797
	30			0.551	0.207	0.159	12.495
	40			0.556	0.211	0.222	19.149

Dynamic anisotropy data for TMA-DPH in DPPC vesicles in the absence and presence of PEG. The phase-resolved dynamic anisotropy data were fit using different models for probe motion, as in Table 2, but always assuming a two-component description of the probe fluorescence lifetime. r_0 was fixed at 0.34. Parameters are defined in Table 2.

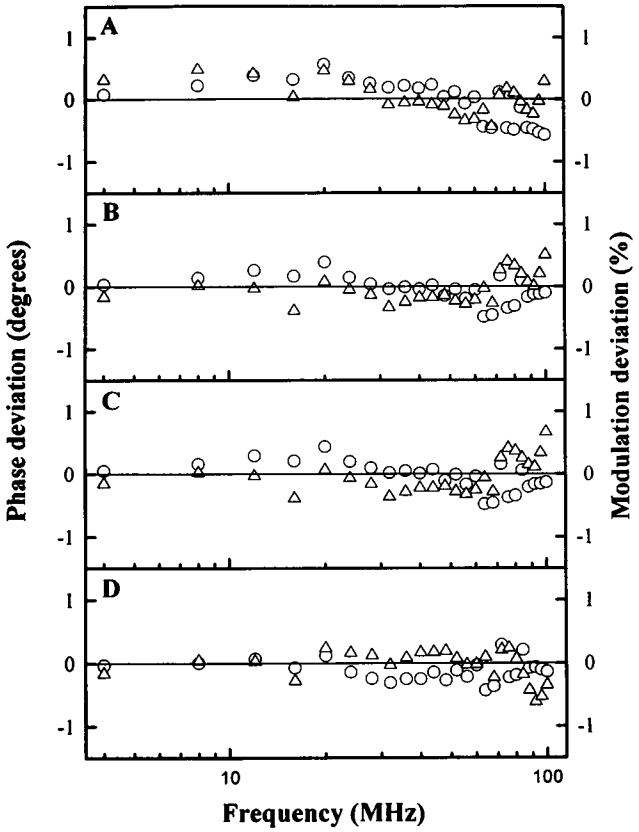

FIGURE 2 Residuals of the fit of frequency-resolved differential phase shifts (*left ordinate*) and modulation ratios (*right ordinate*) for TMA-DPH in DPPC LUV in terms of four possible models: (*A*) free rotation in a cone, with a single average fluorescence lifetime; (*B*) rotation in a P2/P4 orientational potential, with a single average fluorescence lifetime; (*C*) free rotation in a cone, with the dual lifetime components listed in Table 1;, and (*D*) rotation in a P2/P4 orientational potential, with the dual lifetime components listed in Table 1. The parameters and reduced χ^2 values derived from global fits of two such data sets are given in Tables 2 and 3.

imperfect assumption made in deriving the expressions describing TMA-DPH (cylindrical symmetry, excitation and emission dipoles collinear with cylinder axis) could account for this slight mismatch of theory and experiment.

We note that a model that combines "wobble-in-a-cone" motion of a cylindrical probe in a "local cage" with free diffusion of the cage in a P2/P4 orientational potential in the laboratory frame has been described (van der Sijs et al., 1993) and applied to the motion of TMA-DPH (Muller et al., 1994). This most complex model is termed the "combined motion" model, because it purports to recognize that a membrane probe may have a rapid local hindered rotation in a cage combined with the slow rotation of the cage. Although this model has been reported to offer a physically reasonable description of TMA-DPH differential polarized phase and modulation data (Muller et al., 1994), it does so while adjusting five parameters. Given the approximations that must be made to treat the motion of TMA-DPH, this level of complexity seems unjustified, and we treat TMA-DPH motion as free rotation in a limiting cone. This model, when combined with the two resolvable lifetime components, provides a good description of TMA-DPH motion in DPPC LUV and in a variety of other lipid bilayers of varying degrees of unsaturation and curvature (J. Lee, W. Talbot, and B. Lentz, unpublished).

When PEG was included in the LUVET samples, neither the cone nor the P2/P4 model could adequately describe the differential polarized phase and modulation data (Tables 2 and 3), probably because of the strong scattering contribution from samples containing PEG. Because the behavior of TMA-DPH steady-state fluorescence anisotropy that distinguishes fusing from nonfusing membranes occurs only at high PEG concentration, it was impossible to determine the origin of this behavior in terms of either the rate of rotation or a molecular order parameter.

In summary, we can determine from the behavior of fluorescence probes only that a probe sensitive to membrane structure or lipid packing in the bilayer interface region reports a difference between fusogenic and nonfusogenic membranes at PEG concentrations that induce fusion. Unfortunately, these results are obscured by our inability to define more precisely the structural differences between fusogenic and nonfusogenic membranes in the presence of PEG and by the fact that the reporting probe is present in the membrane at concentrations comparable to those of the perturbing amphipaths.

Effects of amphipaths on surface dielectric

It has been hypothesized (Ohki and Arnold, 1990) that a critical event leading to fusion is reduction of the "surface dielectric" reported by the probe DPE to an effective critical value (~12). This probe presumably reflects the polarity of the environment near the glycerol backbone or interface region of the bilayer. Fusogenic concentrations of calcium ions are reported to reduce the surface dielectric of phosphatidylserine membranes, as fusogenic concentrations of PEG are purported to do for phosphatidylserine membranes (Ohki and Arnold, 1990). However, we have shown that, although high concentrations (30–40 wt%) of PEG can bring about molecular contact between membranes (Burgess et al., 1992) or vesicle rupture (Massenburg and Lentz, 1993), even these concentrations will not induce fusion of DPPC LUVET unless other conditions, such as the presence of certain amphipaths, are met (Lentz et al., 1992). To test whether the presence of fusogenic amphipaths might favor fusion by altering the surface dielectric in the presence of PEG, we applied the procedure and fluorescent probe (DPE) used by Ohki and Arnold (1990) to DPPC LUVET containing fusogenic and nonfusogenic amphipaths (Lentz et al., 1992). The results (summarized in Fig. 3) showed that there was no significant difference between the effects of PEG on membranes containing fusogenic (*inverted triangles and squares*) versus nonfusogenic (*triangles and diamonds*) amphipaths. If anything, the presence of fusogenic amphipaths might have slightly mediated the previously

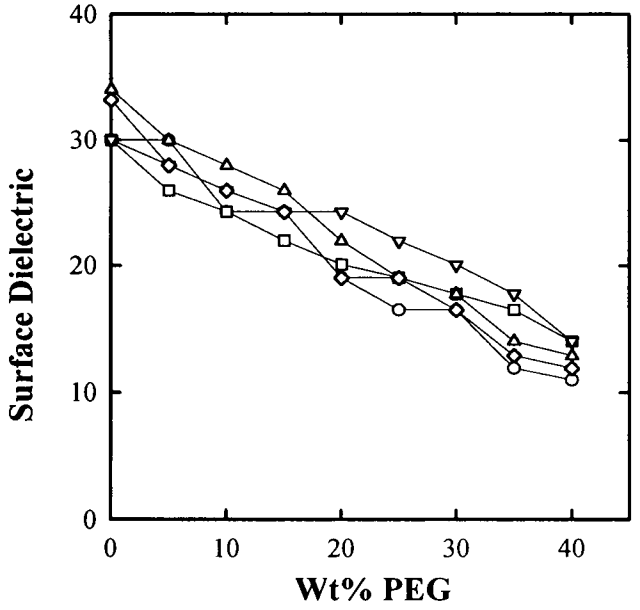

FIGURE 3 Position of the maximum in the fluorescence emission spectrum of DPE in different vesicle membranes (lipid/DPE ~250; lipid concentration 0.05 mM) as a function of PEG concentration. Data are presented for DPPC vesicles alone, or DPPC vesicles containing 0.5 mol% LPC, DOG, PA, and OAG, with symbols as shown in Fig. 1.

noted (Ohki and Arnold, 1990) and anticipated ability of PEG to lower the surface dielectric of DPPC membranes. We conclude that the surface dielectric hypothesis of Ohki and Arnold (1990) cannot account for the structural perturbation key to PEG-mediated fusion.

Lipid internal vibrations by FTIR spectroscopy

Vibrational spectroscopy is an increasingly useful means of detecting and locating membrane structural changes without the use of foreign probes. We have collected FTIR spectra every 2°C from 20 to 40°C, every 1°C from 40 to 43°C, and every 2°C from 43 to 55°C from DPPC LUVETs containing various amphipaths and have focused our attention on the peaks associated with five distinct vibrations associated with the three major regions of the bilayer: the hydrophobic acyl chain region (CH_2 symmetrical stretching at 2850 cm^{-1}; Fig. 4 *A*); the polar headgroup region (PO_4^- antisymmetrical stretching at 1230 cm^{-1}, Fig. 4 *B*; choline C-N-C asymmetrical stretching at 971 cm^{-1}, Fig. 4 *C*); and the interface or glycerol backbone region (C=O stretching at 1734 cm^{-1}, Fig. 4 *D*; C-O-C asymmetrical stretching at 1170 cm^{-1}, Fig. 4 *E*). Assignment of these motions to particular features of the FTIR spectrum of DPPC model membranes has been presented in the liturature along with discussions of the use of these bands to probe bilayer structure (Casal and Mantsch, 1984).

The frequencies of the two CH_2 stretching modes are sensitive to the average rotational conformation about C-C bonds in the phospholipid acyl chains, and thus to the membrane order-disorder phase transition (Mendelsohn and

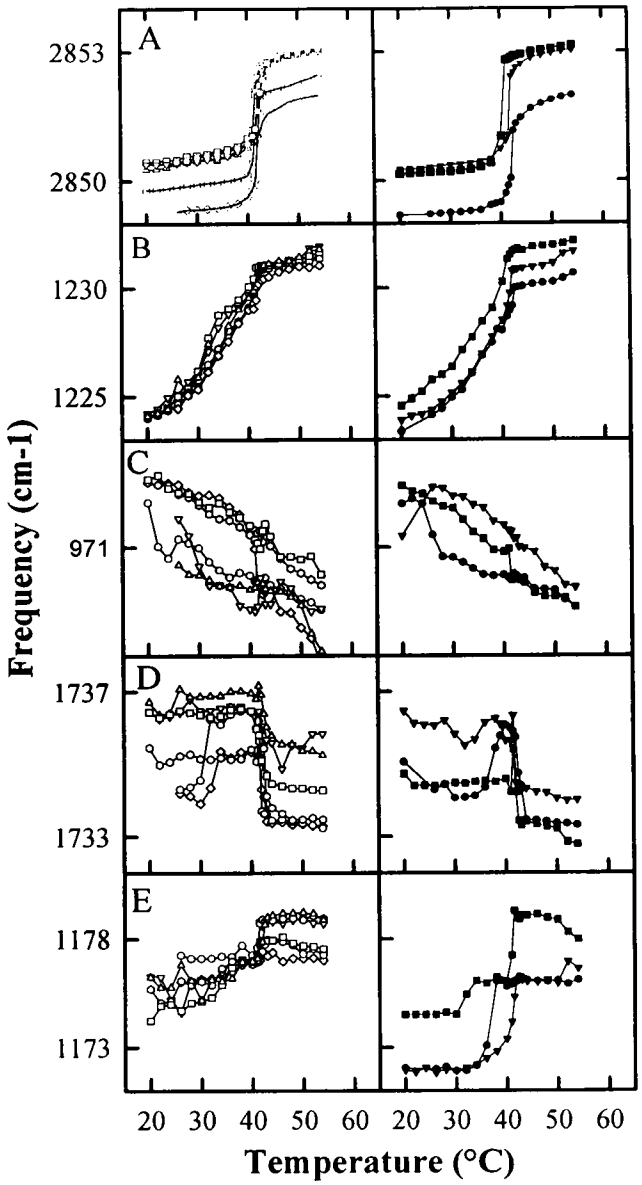

FIGURE 4 Temperature dependence of components of the FTIR spectra of DPPC LUVET containing small amounts of amphipaths (*left panels*: non-fusing membranes; *right panels*: fusing membranes). (*A, left*) Temperature dependence of the CH_2 symmetrical stretching mode in pure DPPC (◇) membranes, and DPPC membranes containing 5 mol% DPG (○), 0.5 mol% DOG (▽), 0.5 mol% OAG (+), 5 mol% MOG (□), and 0.5 mol% stearyl amine (△). (*A, right*) membranes containing 0.5 mol% PA (●), 0.5 mol% L-α-lysophosphatidylcholine (▼), and 5 mol% PAF (■). (*B*) Temperature dependence of the phosphate antisymmetrical stretching mode. (*C*) Temperature dependence of the choline head group C-N-C asymmetrical stretching mode. (*D*) Temperature dependence of the carbonyl group C=O stretching mode. (*E*) Temperature dependence of the ester C-O-C asymmetrical stretching mode. Symbols and panels for *B*, *C*, *D*, and *E* are the same as in *A*.

Mantsch, 1986). Fig. 4 *A* shows the frequency of the symmetrical streching motion in DPPC LUVET plotted as a function of temperature. As expected, the CH_2 stretch is exquisitely sensitive to the main order-disorder phase transition (Mendelsohn and Mantsch, 1986), but there is no

detectable difference in the behavior of this stretching mode between membranes containing fusogenic amphipaths and DPPC membranes containing no amphipaths or nonfusogenic amphipaths. Data for nonfusogenic membranes (*left*) were indistinguishable in their basic behavior from data for membranes containing fusogenic amphipaths (*right*). It is worth noting, however, that all perturbants except PA increased the number of *gauche* C-C bonds in both the fluid and solid phases. The stretching vibrations of the phosphate headgroup (Fig. 3 *B*) also sense the main phase transition, although not as dramatically as the CH_2 stretch. Again, there was no significant difference in the behavior of this vibrational mode between fusogenic (Fig. 4 *B, right*) and nonfusogenic membranes (*left*). Unlike the phosphate and CH_2 motions, the choline headgroup C-N-C asymmetrical stretch showed no sensitivity to the order-disorder phase transition (Fig. 4 *C*). As for the phosphate and CH_2 motions, however, the temperature dependence of this peak frequency was also unaltered by the presence of fusogenic amphipaths in the membrane.

By contrast to the behaviors of these three internal motions of the DPPC molecule, there were differences in the temperature dependencies of the frequency of the C=O stretching (Fig. 4 *D*) and of the C-O-C asymmetrical stretch (Fig. 4 *E*) between fusogenic and nonfusogenic membranes (*right and left panels*, respectively, in these figures). In the case of the C=O stretch, there was for two nonfusing systems (DPPC, *open diamonds*; DPG/DPPC, *open circles*) a dramatic increase in frequency roughly at the temperature of the pretransition, followed by a decrease in frequency as samples were heated through their main phase transition. For membranes containing a dipalmitoyl glycerol (DPG) core, it seems that the rearrangement of bilayer packing occurring at the pretransition affected the glycerol moiety. For other nonfusing samples, the resonance frequency was essentially constant with temperature through the pretransition region, then decreased through the main phase transition. For some nonfusogenic samples there was a slight upward spike in frequency (0.1–0.2 cm^{-1}) just before the decrease. In the case of fusogenic membranes, this spike was much more significant (0.6–1.7 cm^{-1}) and was preceded by a slight (PAF, *closed squares*) or more dramatic (LPC, PA) decrease in frequency just below the main transition. Although we cannot give a simple interpretation of this difference between fusogenic and nonfusogenic membranes, it is clear that this feature consistently correlates with membrane fusogenicity. In the case of the C-O-C asymmetrical stretch (Fig. 4 *E*), the difference between fusogenic (*right*) and nonfusogenic (*left*) membranes was even more clear. This asymmetrical stretching motion within the backbone regions of the DPPC molecule is sensitive to the rearrangements of molecular packing that occur at the main order/disorder phase transition, as evidenced by the jump in frequency that accompanies this phase transition in many of these systems. Whereas the frequency of this motion in many nonfusing DPPC LUVETs showed a slight jump (~1 cm^{-1}) through the main transition, it increased dramatically (~4 cm^{-1}) at T_M in all fusing membranes. Apparently the sensitivity of backbone motions to the order/disorder phase transition is much greater in membranes predisposed to fuse than in membranes that do not fuse in the presence of PEG.

Membrane phase behavior

The FTIR data summarized above suggest that some feature of the molecular packing or structure in the interface region is altered in membranes containing fusogenic amphipaths, in ways that show up at or near the main phase transition temperature. To view this possibility from another perspective, we monitored the thermal phase behavior of DPPC membranes using DSC methods. Although calorimetric determination of the phase behavior of different-sized DPPC vesicles made by extrusion has been reported previously (Lentz et al., 1992), we include for comparison a DSC scan for pure DPPC LUVETs in Fig. 5 (*trace G*). As we have noted previously (Lentz et al., 1992), the melting profile of these vesicles appeared to consist of at least two superimposed peaks (a major component at 41.1°C and a minor component at 41.4°C), with a combined enthalpy of 11.3

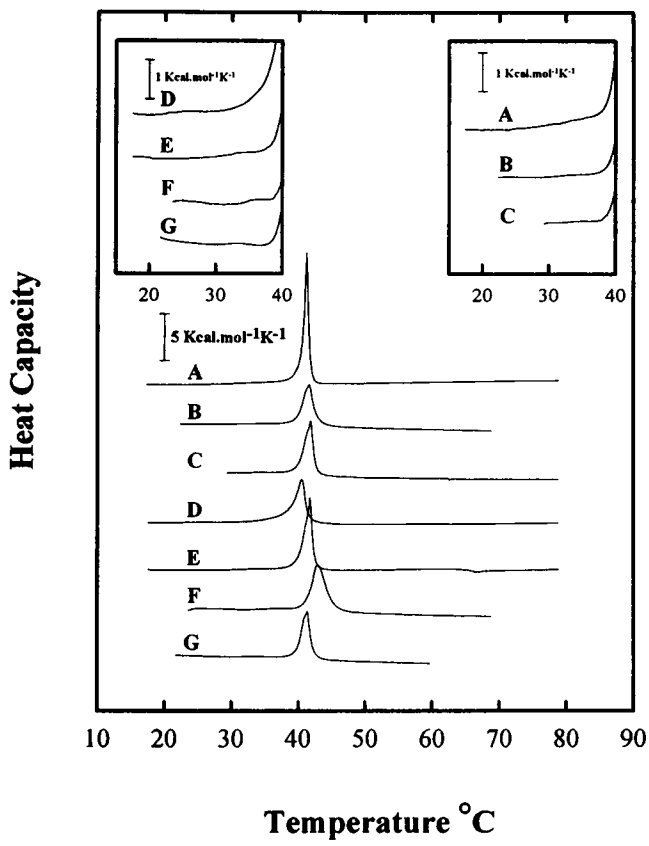

FIGURE 5 Heat capacity endotherms of DPPC LUVETs containing different amphipathic perturbants. *Profile A*, 5 mol% PAF; *B*, 0.5 mol% PA; *C*, 0.5 mol% LPC; *D*, 0.5 mol% OAG; *E*, 5 mol% MOG; *F*, 5 mol% DPG; *G*, pure DPPC. Insets show the data on an expanded scale plotted from 15 to 40°C for nonfusogenic (*left*) and fusogenic (*right*) vesicles.

kcal/mol (Fig. 5 *G*). As observed for large, unilamellar vesicles made by detergent dialysis (Parente and Lentz, 1984), the "pre" or $L_{\beta'} \rightarrow P_{\beta'}$ transition at 35–36°C has a much smaller enthalpy change (~470 cal/mol) than is observed for large, multilamellar vesicles (~1500 cal/mol; Parente and Lentz, 1984).

The inclusion of amphipaths in DPPC LUVETs can be seen to alter their phase behavior (Fig. 5). The main phase transition was shifted to either a higher or lower temperature, but there was no correlation between this shift and the fusogenic potential of the amphipath, as determined previously (Lentz et al., 1992). Similarly, there was no correlation detected between amphipath-induced changes in transition width and fusogenic capability of the amphipath. For membranes that did not fuse in the presence of PEG, a pretransition could be detected, and it was shifted in all cases but one (DPG, *scan F*) to lower temperatures relative to the main transition temperature (Fig. 5, *left-hand inset*). However, a pretransition endotherm could not be detected in membranes containing those amphipaths capable of supporting PEG-mediated vesicle fusion (Fig. 5, *right-hand inset*). It may be that the presence of fusogenic amphipath eliminated the enthalpy associated with this solid-solid phase transition, or that it eliminates or destabilizes the $P_{\beta'}$ phase altogether. Nonfusogenic amphipaths did not have this effect.

The $L_{\beta'} \rightarrow P_{\beta'}$ transition appears to arise from a delicate balance between favorable acyl chain packing in the $L_{\beta'}$ phase and enhanced bilayer hydration in the $P_{\beta'}$ phase (Parsegian, 1983; Cevc, 1991). Acyl chains remain fully extended in both phases, but are less closely packed and are free to rotate about their long axis in the $P_{\beta'}$ phase (Boroske and Trahms, 1993). The lost enthalpy from decreased chain-chain interaction is balanced in the $P_{\beta'}$ phase by the increased free energy of hydration of head and interface regions of the bilayer (Parsegian, 1983; Cevc, 1991). Thus, the pretransition shifts toward the chain-melting, main transition with decreased water activity in the bathing medium, creating a triple point at a critical water activity (Wack and Webb, 1988; Cevc, 1991). According to the treatment of Cevc (1991), the driving force for the pretransition is the ability of the interface region to swell and admit water molecules. Thus the $P_{\beta'}$ phase will be destabilized relative to $L_{\beta'}$, and the transition will be shifted to the main transition by anything that increases the interfacial tension between the hydrocarbon and water phases in the interfacial or backbone region of the bilayer. Apparently all three fusogenic amphipaths examined create some change in the structure of the interface region of the bilayer that has this effect (Fig. 5, *right*).

CONCLUSIONS

1. Three types of measurements (motional properties of fluorescent probes; temperature dependence of vibrational modes detected by FTIR spectroscopy; membrane phase behavior as detected by DSC) point to changes in the structure of the interface region of the bilayer as a common feature distinguishing the perturbing influence of fusogenic amphipaths from the influence of nonfusogenic amphipaths. Although located by our observations in the interface region, the detailed molecular nature of this structural change cannot be defined at this time.

2. Whatever the structural change induced by fusogenic amphipaths in DPPC LUVETs, the disappearance of the pretransiton detected by DSC suggests that it makes water penetration into the interface region thermodynamically less favorable. This perturbing influence of fusogenic amphipaths could result in destabilization of the bilayer state, leading to the formation of a fusion intermediate between closely apposed bilayers.

3. There is no correlation between structural perturbations induced by amphipaths in the hydrophobic core or the headgroup regions of the bilayer and amphipath fusogenicity.

4. Despite the implications of our results for the importance to fusion of the structure and hydration of the bilayer interface region, there is no correlation between PEG-mediated fusion and the PEG-induced change in the effective dielectric constant of the water layer at the membrane surface, as had been suggested by Ohki and Arnold (1990).

In a recent study of DPPC LUVETs made highly fusogenic by an asymmetrical distribution of LPC (Wu et al., 1996), we suggested that the key event promoting fusion was loosening of the lipid packing in the contacting or outer leaflets of two membranes brought into close apposition by PEG. Lipid packing disruption should create a high free energy state that would favor the formation of a fusion intermediate. This hypothesis is certainly consistent with the conclusions reached here, because the structure of the interface region should be most sensitive to alterations in bilayer packing density.

Supported by USPHS grant GM32707 to BRL.

REFERENCES

Boroske, E., and L. Trahms. 1993. A ^{1}H and ^{13}C NMR study of motional changes of dipalmitoyllecithin associated with the pretransition. *Biophys. J.* 42:275–283.

Burgess, S. W., D. Massenburg, J. Yates, and B. R. Lentz. 1991. Poly(ethylene glycol)-induced lipid mixing but not fusion between synthetic phosphatidylcholine large unilammelar vesicles. *Biochemistry.* 30: 4193–4200.

Burgess, S. W., T. J. McIntosh, and B. L. Lentz. 1992. Modulation of poly(ethylene glycol)-induced fusion by membrane hydration: importance of interbilayer separation. *Biochemistry.* 31:2653–2661.

Casal, H. L., and H. H. Mantsch. 1984. Polymorphic phase behavior of phospholipid membranes studied by infrared spectroscopy. *Biochim. Biophys. Acta.* 779:381–401.

Cevc, G. 1991. Polymorphism of the bilayer membranes in the ordered phase and the molecular origen of the lipid pretransition and rippled lamellae. *Biochim. Biophys. Acta.* 1062:59–69.

Chen, L. A., R. E. Dale, S. Roth, and L. Brand. 1977. Nanosecond time-dependent fluoresecnce depolarization of diphenylhexatriene in

dimyristoyllecithin vesicles and the determination of "microviscosity." *J. Biol Chem.* 252:2163–2169.

Chen, P. S., Jr., T. Y. Toribara, and H. Warner. 1956. Microdetermination of phosphorus. *Anal. Chem.* 28:1756–1758.

Chernomordik, L., A. Chanturiya, J. Green, and J. Zimmerberg. 1995. The hemifusion intermediate and its conversion to complete fusion: regulation by membrane composition. *Biophys. J.* 69:922–929.

Chernomordik, L. V., S. S. Vogul, A. Sokoloff, H. O. Onaran, E. A. Leikina, and J. Zimmerberg. 1993. Lysolipids reversibly inhibit Ca^{2+}, GTP and pH dependent fusion of biological membranes. *FEBS Lett.* 318:71–76.

Ho, C., S. J. Slater, and C. D. Stubbs. 1995. Hydration order in lipid bilayers. *Biochemistry.* 34:6188–6195.

Kinosita, K., Jr., S. Kawato, and A. Ikegama. 1977. A theory of fluorescence depolarization decay in membranes. *Biophys. J.* 20:289–305.

Lentz, B. R. 1993. Use of fluorescent probes to monitor molecular order and motions within liposome bilayers. *Chem. Phys. Lipids.* 64:99–116.

Lentz, B. R. 1994. Polymer-induced membrane fusion: potential mechanism and relation to cell fusion events. *Chem. Phys. Lipids.* 73:91–106.

Lentz, B. R., G. F. McIntyre, D. J. Parks, J. C. Yates, and D. Massenburg. 1992. Bilayer curvature and certain amphipaths promote poly(ethylene glycol)-induced fusion of dipalmitoyl phosphatidylcholine unilamellar vesicles. *Biochemistry.* 61:2643–2653.

Massenburg, D., and B. R. Lentz. 1993. PEG-induced fusion and rupture of dipalmitoylphosphatidylcholine large unilamellar vesicles. *Biochemistry.* 32:9172–9180.

Mayer, L. D., M. J. Hope, and P. R. Cullis. 1986. Vesicles of variable sizes produced by a rapid extrusion procedure. *Biochim. Biophys. Acta.* 858: 161–168.

Mendesohn, R., and H. H. Mantsch. 1986. Fourier transform infrared studies of lipid-protein interactions. *In* Progress in Protein-lipid Interactions, Vol. 2. A. Watts and J. J. H. DePont, editors. Elsevier Science Publishers, New York. pp. 103–146.

Muller, J. M., E. van Fassen, and G. van Ginkel. 1994. Experimental support for a novel compound motion model for the time-resolved fluorescence anisotropy decay of TMA-DPH in lipid vesicle bilayers. *Chem. Phys.* 185:394–404.

Ohki, S., and K. Arnold. 1990. Surface dielectric constant, surface hydrophobicity, and membrane fusion. *J. Membr. Biol.* 114:195–203.

Parente, R. A., and B. R. Lentz. 1984. Phase behavior of large unilamellar vesicles composed of synthetic phospholipids. *Biochemistry.* 23: 2353–2362.

Parsegian, V. A. 1983. Dimensions of the "intermediate" phase of dipalmitoylphosphatidylcholine. *Biophys. J.* 44:413–414.

Straume, M., and B. J. Litman. 1987. Equilibrium and dynamic structure of large, unilamellar, unsaturated acyl chain phosphatidylcholine vesicles. Higher order analysis of 1,6-diphenylhexatriene anisotropy decay. *Biochemistry.* 26:5113–5120.

van der Meer, W., H. Pottel, W. Herreman, M. Ameloot, H. Hendrickx, and H. Schroder. 1984. Effect of orientational order on the decay of the fluorescence anisotropy in membrane suspensions. *Biophys. J.* 46: 515–523.

van der Sijs, D. A., E. E. van Faassen, and Y. K. Levine. 1993. On the interpretation of fluorescence anisotropy decays of probe molecules in membrane systems. *Chem. Phys. Lett.* 216:559–565.

van Langen, H., G. van Ginkel, D. Shaw, and Y. K. Levine. 1989. The fidelity of response by 1-[4-(trimethylammonio)phenyl]-6-phenyl-1,3,5-hexatriene in time-resolved fluorescence anisptropy measurements on lipid vesicles. *Eur. Biophys. J.* 17:37–48.

Wack, D. C., and W. W. Webb. 1988. Measurements of modulated lamellar $P_{\beta'}$ phases of interacting lipid membranes. *Phys. Rev. Lett.* 61: 1210–1213.

Wang, S., J. M. Beechem, E. Gratton, and M. Glaser. 1991. Orientational distribution of 1,6-diphenyl-1,3,5-hexatriene in phospholipid vesicles as determined by global analysis of frequency domain fluorimetry data. *Biochemistry.* 30:5565–5572.

Wu, H., L.-X. Zheng, and B. R. Lentz. 1996. A slight asymmetry in the transbilayer distribution of lysophosphatidylcholine alters the surface properties and PEG-mediated fusion of dipalmitoylphosphatidylcholine large unilamellar vesicles. *Biochemistry.* 38:12602–12611.

Zannoni, C., A. Arcioni, and P. Cavatorta. 1983. Fluorescence depolarization in liquid crystals and membrane bilayers. *Chem. Phys. Lipids.* 32:179–250.